The average response was, therefore, difficult to measure and the shape of the concentration-response curves is less reliable.
14. M. E. Maguire and J. J. Erdos, *J. Biol. Chem.* **255**, 1030 (1980).
15. We thank V. Pirrotta for bringing the T7 polymerase-promoter expression system to our attention and to S. Tabor for making pT7-7, mGP1-2, pGP1-2, and their documentation available to us. Supported in part by NIH grants DK-19318 and HL-31164 to L.B., HL-39262, HL-37044, and NS-23877 to A.M.B., EY-02423 and EY-02608 to D. Lam, GM-34497, American Cancer Society grant BC-5551, and the Raymond and Ellen Willie Chair of Molecular Neuropharmacolgy to A.G.G., and the NIH Diabetes and Endocrinology Center grant DK-27685 to Baylor College of Medicine (J. B. Field, director).

29 June 1988; accepted 23 November 1988

Stretch-Inactivated Ion Channels Coexist with Stretch-Activated Ion Channels

CATHERINE E. MORRIS AND WADE J. SIGURDSON

Stretch-activated ion channels of animal, plant, bacterial, and fungal cells are implicated in mechanotransduction and osmoregulation. A new class of channel has now been described that is stretch-inactivated. These channels occur in neurons, where they coexist with stretch-activated channels. Both channels are potassium selective. The differing stretch sensitivities of the two channels minimize potassium conductance over an intermediate range of tension, with the consequence that, over this same range, voltage-gated calcium channels are most readily opened. Thus, by setting the relation between membrane tension and transmembrane calcium fluxes, stretch-sensitive potassium channels may participate in the control of calcium-dependent motility in differentiating, regenerating, or migrating neurons.

STRETCH-ACTIVATED (SA) CHANNELS have been studied in diverse cell types (*1–4*). In snail neurons, under conditions used to study SA K^+ channels (*5, 6*), some membrane patches were observed in which suction through the recording pipette not only activated the ubiquitous SA channels, but simultaneously inhibited a class of lower conductance, spontaneously active channels. In a single-channel recording where SA channel activity was abolished by quinidine, spontaneous currents (multiples of ~1 pA) were evident in the absence of external membrane tension and were abolished by suction (Fig. 1A). By contrast, more typical patches of membrane did not exhibit stretch-inactivated (SI) currents (*7*) but were nearly quiescent until stretch evoked SA channel activity (Fig. 1B). We suspect that even with the pipette tip tension nominally at zero, there was often sufficient residual suction (from capillarity) to inactivate the SI channels. This would explain why it was sometimes possible to stimulate activity by applying 3 to 5 mmHg of positive pressure; this activity subsided with further positive pressure, as expected for an SI channel. The occurrence of SI and SA (*8*) currents together (Fig. 1, C, D, and E) in a single patch from cell bodies or growth cones demonstrates that distinct populations of channels with reciprocal responses to mechanical tension can coexist within a membrane area of several square micrometers.

To exclude the possibility that suction inhibits channel activity not because of increased membrane tension but because the channel-bearing membrane is drawn against the inner wall of the pipette, amplitude histograms were examined for the presence of attenuated events. Under conditions where suction sharply decreased the open probability (P_o) for SI channels, the distribution of single channel amplitudes was unchanged (Fig. 2). Calcium-related artifacts (for example, Ca^{2+} inactivation induced by inward leak of Ca^{2+}) are ruled out by the observation of SI events in Ca^{2+}-free conditions (Fig. 3). Even with such artifacts eliminated, do membranes in fact encounter tensions comparable to those applied through the patch pipette? Probably they do; for a semipermeable membrane, a mere 1 mos*M* equals 18 mmHg. Moreover, at the advancing tip of crawling cells, motility generates forces ranging from 10^{-8} to 10^{-3} dyne/μm (*9*), so that experimental tensions [on the order of 10^{-5} to 10^{-4} dyne/μm for −10 mmHg in a typical patch (*1*)] are not excessive.

For the SI channel, as for the SA channel (*5*), analysis of single-channel current-voltage relations indicates that K^+ is the physiologically permeant species. With normal saline (NS) in the pipette (Fig. 3), the zero-current potential for the SI channel was near the resting potential and, as expected for a channel with negligible Na^+ and intracellular anion permeability, the channel did not pass inward current. When Na^+ was re-

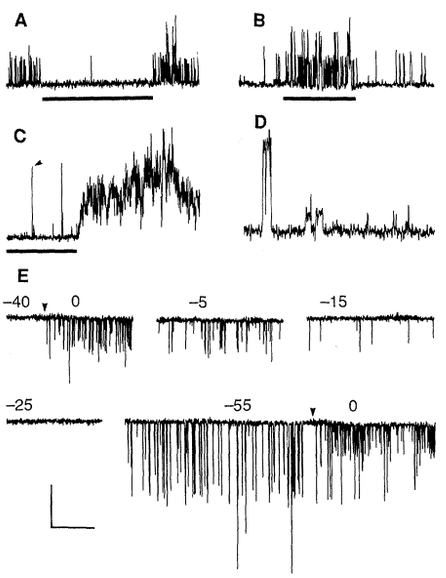

Fig. 1. Currents inhibited and activated by membrane stretch coexist. (**A**) Activity of SI channels in a cell body patch abolished by application of about −40 mmHg. NS plus 1 m*M* quinidine (*18*) in pipette; membrane potential, V_m = +70 mV. (**B**) SA channel activity stimulated by −40 mmHg. NS in pipette; V_m = +70 mV. Sustained responses in (A) and (B) were typical; note different amplitude calibration. (**C**) SA channel (arrowhead) and SI channel activity in the same patch, −70 mmHg, NS in pipette, V_m = +70 mV. (**D**) Higher resolution trace of SA channel and SI channel events from a growth cone, 0 mmHg, 50 m*M* K^+ in pipette, patch V_m = V_{rest} + 120 mV (the resting potential, V_{rest}, was unknown for growth cones). (**E**) SI and SA channels in a growth cone patch. Suction (in millimeters of mercury) is indicated adjacent to each segment of record; at the arrowheads, suction was abruptly released. Note that between about −20 and −50 mmHg, neither channel type was active. Fifty millimolar KCl in the pipette; patch held at V_{rest}. Calibration: (A) 1 pA, 2 s; (B) 4 pA, 2 s; (C) 2 pA, 1 s; (D) 2 pA, 40 ms; (E) 4 pA, 2 s. Traces (A), (B), (D), and (E) filtered at 1 kHz, (C) at 500 Hz. Solid bars below traces (here and in Fig. 3) indicate suction. *Lymnaea stagnalis* neurons were isolated from circumesophageal ganglia (45 min in 0.25% protease), plated on glass cover slips, and used for up to 4 days after dissociation. Cells were maintained in NS (50 m*M* NaCl, 1.6 m*M* KCl, 3.5 m*M* $CaCl_2$, 2 m*M* $MgCl_2$, 5 m*M* Hepes, *p*H 7.6) supplemented with 5 m*M* glucose, 50 IU of penicillin per milliliter, and 50 μg of streptomycin per milliliter. All recordings were made on cells bathed in this solution (exception noted in Fig. 3) at room temperature. Patch-clamp recordings of single-channel activity were made with standard cell-attached gigaseal techniques (*19*); pipettes were made from Corning 7052 glass. Suction, applied through a port in the microelectrode holder, was measured and controlled with a Bio-tek transducer. Cell body membrane potentials are calculated on the assumption of V_{rest} = −50 mV [from intracellular recordings, V_{rest} = −51 ± 1.9 mV (SEM), n = 32].

Department of Biology, 30 Somerset Street East, University of Ottawa, Ottawa, Ontario, Canada K1N 6N5.

placed with K^+ (making no Cl^- changes), inward SI currents were seen at rest (three patches), and the reversal potential (V_{rev}) shifted to ~0 mV. The current-voltage relations of a Cl^- channel would not be altered by this cation substitution. Since inward and outward SI currents were seen with thallium acetate (TlAc) in the pipette (Fig. 3), the possibility that the SI channel is anion-selective is ruled out unless extracellular TlAc inexplicably induces permeability to intracellular anions. SI currents were also observed with 50 m*M* RbCl in the pipette; as with K^+ and Tl^+, V_{rev} shifted in the depolarizing direction (to −12 mV), with 0.5 pA SI inward Rb^+ currents at the resting membrane potential (V_{rest}) and outward K^+ currents at positive potentials. These permeation characteristics (that is, substantial conductance for Tl^+ followed by K^+ and Rb^+, and sparing or zero permeability to Na^+ and anions) are consistent with properties shown for other highly K^+ selective channels (*10*) including *Lymnaea* SA channels (*5*). Recently, SA channels with similar permeation properties have been described in vertebrate cells (*11, 12*).

On three cell body patches (different cells), we measured P_o for SI channels at four or more pressures. In each case, P_o descreased to 50% or less (compared to 0 mmHg) by −15 mmHg. By contrast, SA channel activation in *Lymnaea* neurons seldom attained a half maximal level before −30 mmHg. The stretch sensitivity of SI and SA channels in a cell body patch and in two growth cone patches is shown in Fig. 4. The "notch-filter" appearance of the paired curves (that is, SI/SA activity from the same patch) of Fig. 4 is particularly noteworthy because it shows how intermediate tensions minimize K^+ permeability, thereby maximizing the likelihood of membrane excitation and the attendant entry of Ca^{2+} through voltage-gated Ca^{2+} channels. Given the central role of Ca^{2+} in the control of exocytosis, of cytoskeletal structure, and of growth cone motility (*13, 14*), membrane tension effects on SI and SA channel activity could have important feedback consequences for local motility and for morphology. It is plausible that reduced adhesion to the substrate would activate SI channels, whereas excessively rapid growth or abutment against a surface would recruit SA channels. A widespread utilization of mechanosensitive K^+ channels in morphogenesis is suggested by the finding that SA K^+ channels are activated cyclically in dividing vertebrate embryonic cells (*12*).

Stretch-dependent decreases in the SI channel P_o could stem either from stretch-induced increases in the rate of leaving an open state (yielding briefer open sojourns) or from decreases in the rate of leaving a closed state (longer closed sojourns). Open time histograms for SI events could be fit with a single exponential, whereas multiple exponentials were required for the closed times, the longest of which could be ascribed to a "between-bursts" state. Table 1 provides evidence that the channel open time is insensitive to membrane tension. In contrast, the long closed time lengthens with increasing stretch as P_o declines. Interestingly, SA K^+ channels (*2*) and other SA channels (*1, 15*) conform to this same basic

Table 1. Kinetics for SI channels at three pressures. Time constants (τ_{open} and τ_{closed}) obtained from a cell body patch in which the SI channel activity was appropriate for kinetic analysis over a range of pressures including 0 mmHg. Insufficient events precluded multiexponential fits to the closed-time data in this patch, so measurements are restricted to closed times that should belong to the slowest component. NS plus 1 m*M* quinidine in pipette, V_m = +90 mV. For analysis, data were filtered at 2.5 kHz and digitized at 20 kHz.

Pressure (mmHg)	Relative P_o*	τ_{open}† (ms)	τ_{closed}‡ (ms)
0	1	0.85 ± 0.07 (0.87)	109
−15	0.16	1.12 ± 0.29 (0.87)	294
−30	0.068	0.75 ± 0.23 (0.85)	559

*P_o relative to value at 0 mmHg, which was 0.024. †Given both as inverse rate constant (±SEM, the error associated with the fit) to a single exponential fit (events ≥0.1 ms) and (in parentheses) as a maximum likelihood estimate [that is, average open time minus cutoff time of 0.1 ms; see Eq. 50 in (*17*)]. ‡Average closed time minus cutoff time of 5 ms (*17*).

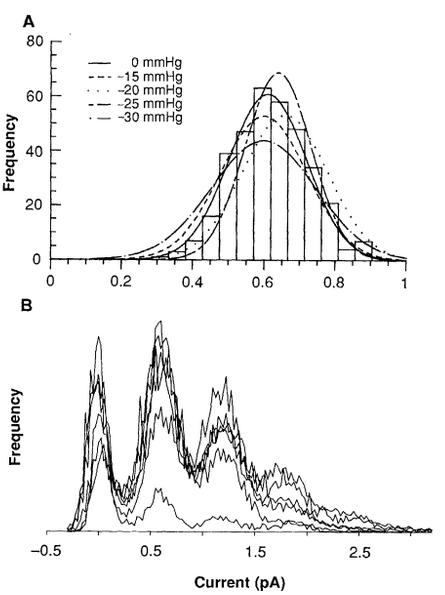

Fig. 2. Suction does not affect elementary SI channel current amplitude. (**A**) Patch in which multiple openings were rare (same as Table 1); histogram (constructed from events used in kinetic analyses) for 0 mmHg is shown. Overlying lines are Gaussian fits to this data and to histograms (not shown) for four other pressures. Suction did not decrease the mean amplitude, and tests for skewness and kurtosis indicated no deviations from Gaussian distributions. (**B**) Patch in which multiple openings were the norm (same as Fig. 4, cell body); family of amplitude histograms (constructed point by point from data filtered at 1 kHz and digitized at 10 kHz) for six pressures ranging from 0 to −30 mmHg show that both within a given histogram and from one pressure to the next, amplitude peaks occur at multiples of 0.6 pA.

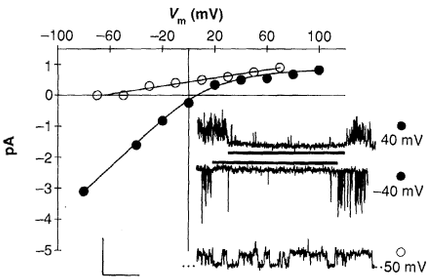

Fig. 3. SI channel current-voltage relations. ○, NS in the pipette; conductance, 6.6 pS (linear regression to all points), zero-current intercept, −66 mV; ●, 50 m*M* TlAc in the pipette, 50 m*M* KCl in bath, both solutions Ca^{2+}-free (2.2 m*M* EGTA in bath only) and buffered with Hepes (5 m*M*), V_{rest} assumed to be 0 mV. Slopes (fit by eye) of linear portions are 38 pS (lower quadrant) and 5.6 pS (upper quadrant), V_{rev} = +7 mV. Note that the outward current conductances with NS and TlAc in the pipette are similar, suggesting that intracellular K^+ carries the current in both cases. (Inset) Stretch inactivation (~40 mmHg) of outward and inward currents (TlAc experiment), and (bottom), at a higher time resolution, a record from the NS experiment, V_m as indicated. Cell body patches for both experiments. Calibration: 2 pA, 4 s (top traces), 40 ms (bottom trace).

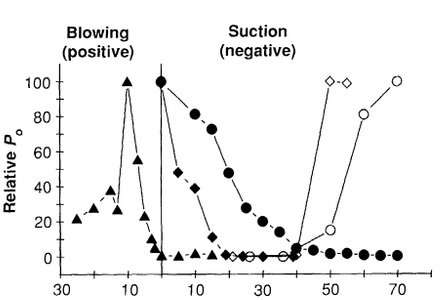

Fig. 4. SI and SA channels coexist in patches from cell body and growth cone. Ordinate, P_o normalized to the maximum value for each type of channel in each patch; solid symbols refer to SI channels, open symbols to SA channels. ○, ●, Paired curves for a cell body patch (same patch as Fig. 1C); ◇, ◆, paired curves for a growth cone patch. ▲, As explained in text, growth cone SI channels with activity that was suppressed by the residual pipette suction (−10 mmHg); note inactivity at nominally zero and negative pressures. ○, ●, NS in pipette, V_m = +70 mV; ◇, ◆, 50 m*M* K^+ in pipette, patch at V_{rest} (same patch as Fig. 1E); ▲, 50 m*M* K^+ in pipette, patch $V_m = V_{rest} - 60$ mV.

pattern: stretch acts on the between-bursts closed time, without substantially altering either open times or brief closed times. In stretch-sensitive channels, therefore, slow mechanical transduction processes and fast kinetic processes may represent modes of gating arising from spatially distinct regions of the channel.

Several additional observations on SI channels are worth noting. The maximum number of SI channels in any patch was ten and the minimum in patches that exhibited SI events was two, a range corresponding to that for SA channels in *Lymnaea* neurons. (Density per patch is obtained from the maximum number of stretch-sensitive elementary amplitudes, as seen in Fig. 2B). SI channels, like SA channels, showed no obvious voltage dependence; spontaneous SI channel activity at V_{rest} was evident with K^+, Tl^+, or Rb^+ in the pipette and no inactivation occurred with depolarization. Normal-looking SI events were observed with both 10 m*M* tetraethylammonium and 1 m*M* quinidine (for example, Fig. 1A) in the pipette. The phenomenon of channel inactivation by stretch is not unique to this preparation; SI channels have been observed in mammalian astrocytes (*16*).

A number of properties shared by the two stretch-sensitive channels (the parallel kinetic effects of stretch on a between-bursts closed state in both, the similarities in membrane densities, the concurrent changes of SI and SA activity in a given patch) are consistent with the possibility that the channels are linked to a common transduction mechanism. A good candidate is the submembranous filament network proposed by Sachs (*3*). The discovery of an SI channel in parallel with the SA channel also raises the interesting prospect that yet other integral membrane proteins—ones implicated in cell motility, cell compliance, or osmoregulation, but with "outputs" that are not necessarily measurable with a patch clamp (carriers, enzymes)—might also be influenced by membrane tension.

REFERENCES AND NOTES

1. F. Guharay and F. Sachs, *J. Physiol. (London)* **352**, 685 (1984).
2. W. J. Sigurdson, C. E. Morris, B. L. Brezden, D. R. Gardner, *J. Exp. Biol.* **127**, 191 (1987).
3. F. Sachs, *Membr. Biochem.* **6**, 173 (1986); *CRC Crit. Rev. Biomed. Eng.* **16**, 141 (1988).
4. R. Kullberg, *Trends Neurosci.* **10**, 387 (1987); B. Martinac, M. Buechner, A. H. Delcour, C. Kung, *Proc. Natl. Acad. Sci. U.S.A.* **84**, 2297 (1987); M. C. Gustin, X. L. Zhou, B. Martinac, M. R. Culbertson, C. Kung, *Biophys. J.* **51**, 251a (1987); L. Falke, K. L. Edwards, B. G. Picard, S. Misler, *ibid.*, p 251a; O. Christensen, *Nature* **330**, 66 (1987); L. L. Stockbridge and A. S. French, *Biophys. J.* **54**, 187 (1988); M. T. Kirber, J. V. Walsh, Jr., J. J. Singer, *Pfluegers Arch.* **412**, 339 (1988).
5. W. J. Sigurdson *et al.*, *Biophys. J.* **51**, 50a (1987).
6. W. J. Sigurdson and C. E. Morris, *J. Neurosci.*, in press.
7. SI channels were observed in 13 out of 219 patches made on cell bodies with pipettes made from small bore (outside diameter, 1.65 mm; inside diameter, 0.85 mm) tubing. When such pipettes were used on growth cones, SI channel activity was not observed (15 patches), but with wider bore pipettes (outside diameter, 1.65 mm; inside diameter, 1.15 mm), 3 of 11 successfully patched growth cones exhibited SI channels. This frequency of occurrence represents a minimum; it is likely that patches were discarded as being merely "noisy" when in fact they were displaying multiple spontaneously active SI channels. On two cells in which SI channels were noted, second and third patches were obtained. All showed SI and SA currents, indicative, for these cells at least, of a homogeneous channel distribution.
8. SA channel activity was recognized by the outwardly rectifying current-voltage relations [normal saline (NS) in the pipette, cell-attached], by conductance (~30 to 40 pS under these conditions), and by kinetics (brief bursts activated by stretch).
9. A. K. Harris, P. Wild, D. Stopak, *Science* **208**, 177 (1980); M. Dembo and A. K. Harris, *J. Cell Biol.* **91**, 528 (1981).
10. G. Yellen, *Annu. Rev. Biophys. Chem.* **16**, 227 (1987).
11. H. Sackin, *Am. J. Physiol.* **253**, F1253 (1987); *Proc. Natl. Acad. Sci. U.S.A.*, in press.
12. I. R. Medina and P. D. Bregestovski, *Proc. R. Soc. London Ser. B* **235**, 95 (1988).
13. J. G. Augustine, M. P. Charlton, S. J. Smith, *Annu. Rev. Neurosci.* **10**, 633 (1987).
14. S. B. Kater, M. P. Mattson, C. Cohan, J. Connor, *Trends Neurosci.* **11**, 315 (1988); C. S. Cohan, J. A. Connor, S. B. Kater, *J. Neurosci.* **7**, 3588 (1987).
15. J. B. Lansman, T. J. Hallam, T. J. Rink, *Nature* **325**, 811 (1987).
16. F. Sachs, personal communication.
17. D. Colquhoun and F. J. Sigworth, in *Single-Channel Recording*, B. Sakmann and E. Neher, Eds. (Plenum, New York, 1983), pp. 191–263.
18. B. L. Brezden, D. R. Gardner, C. E. Morris, *J. Exp. Biol.* **123**, 175 (1986).
19. O. P. Hamill, A. Marty, E. Neher, B. Sakmann, F. J. Sigworth, *Pfluegers Arch.* **391**, 85 (1981).

20. We thank J. A. Connor and M. D. Schneider for their helpful comments on the manuscript. Supported by the Natural Sciences and Engineering Research Council of Canada and the Muscular Dystrophy Association of Canada.

1 September 1988, accepted 23 November 1988

Nimodipine Facilitates Associative Learning in Aging Rabbits

RICHARD A. DEYO, KAREN T. STRAUBE, JOHN F. DISTERHOFT*

Nimodipine is one of several dihydropyridines that block calcium channels. Originally administered to improve cerebral blood flow in elderly patients with chronic cerebrovascular disorders, nimodipine was noted to facilitate learning. These observations led to the present investigation of the effects of nimodipine on associative learning in aging rabbits. Nimodipine accelerated acquisition of conditioned eye-blink in both young and aging rabbits without altering the amplitude of responses to the conditioned or unconditioned stimuli or causing nonspecific responding. Thus, nimodipine may be a candidate for an effective treatment for age-related learning deficits.

ONE OF THE MOST DEBILITATING consequences of aging can be memory loss. Although many changes occur within the central nervous system during aging (that is, decreases in neurotransmitter synthesis and degradation, decreases in receptor number, and increases in cell loss), the perturbation of normal Ca^{2+} metabolism appears to be an important factor correlated with both the age-related physiological deficits and the learning and memory deficits (*1, 2*).

There is a relation between Ca^{2+} metabolism and selected mechanisms of learning and memory in aged subjects. (i) A Ca^{2+}-activated K^+ current is reduced in hippocampal neurons after associative learning in rabbits (*3*). This same current is prolonged in hippocampal neurons from aging brain and may contribute to the learning deficits that often accompany normal aging (*4*). (ii) The elevation of plasma Mg^{2+} (a competitive inhibitor of many actions of Ca^{2+}) improves reversal learning in both aged and young rats (*5*). (iii) Alterations in normal Ca^{2+} homeostasis in aged subjects, such as an increase in the intraneuronal Ca^{2+} concentration, can also be toxic to neurons (*2, 6*). Hence, Ca^{2+} channel antagonists would be expected to improve learning and memory in aged subjects by decreasing neuronal influx of Ca^{2+}, thereby reducing prolonged Ca^{2+}-activated currents or minimizing Ca^{2+} toxicity in neurons from aged brain. Nimodipine, a potent Ca^{2+} channel blocker (*7*), has been noted to enhance learning and memory in older persons with chronic cerebrovascular disorders (*8*).

Here we have tested the effect of nimodipine on eye-blink conditioning of rabbits. This well-studied behavioral system is useful, because both aged humans and rabbits show similar deficits in the acquisition of this conditioned response (*9, 10*).

Thirty-six experimentally naïve New Zealand albino rabbits (*Oryctolagus cuniculus*) were assigned to one of four treatment groups based on age and drug treatment

Department of Cell Biology and Anatomy, Northwestern University Medical School, Chicago, IL 60611.

*To whom correspondence should be addressed.